Supplementary Material

Vegetation Dynamics and Driving Mechanism Considering Time-Lag and Accumulation Effects: A Case Study of the Hubao-Egyu Urban Agglomeration

Xi Liu[1], Guoming Du[1,*], XiaoDie Zhang[2], Xing Li[1,*], Shining Lv[3], Yinghao He[1]

[1] School of Geography and Planning, Sun Yat-sen University, Guangzhou 510006, China; liux663@mail2.sysu.edu.cn (Xi Liu); eesdgm@mail.sysu.edu.cn (D.G.M.); lixing58@mail.sysu.edu.cn (Xing Li); hyh141592654@163.com (H.Y.H.)

[2] Beidou Research Institute, South China Normal University, Foshan 528225, China; 2023025241@m.scnu.edu.cn

[3] School of Traffic & Transportation Engineering, Changsha University of Science & Technology, Changsha 410114, China; 22201050156@stu.csust.edu.cn

Data are available from the author below, upon reasonable request.

*Corresponding author: Guoming Du. eesdgm@mail.sysu.edu.cn ; Li Xing . lixing58@mail.sysu.edu.cn ;

The First author: Xi Liu. liux663@mail2.sysu.edu.cn

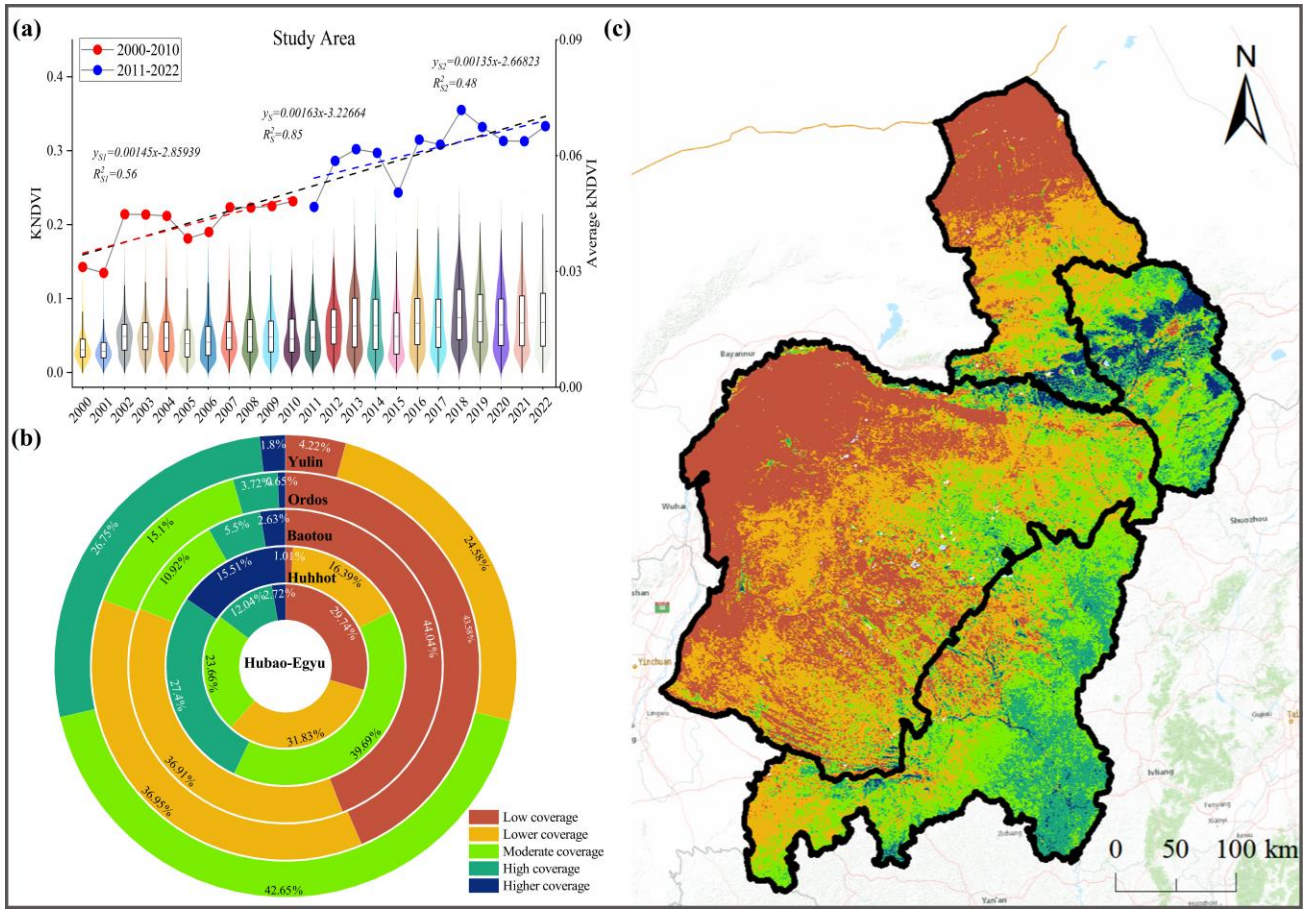

Figure S1. Temporal variation characteristics of kNDVI in HBEY (a). The red and blue dots in the figure represent the average kNDVI, and the violin plot shows the distribution of kNDVI in a given year. The whisker of the violin diagram represents the data range, and the upper boundary, horizontal line, and lower boundary of the box part represent the upper, median, and lower quartile of the data, respectively. The width of the violin map reflects the data density at that location. According to the natural break method, the average kNDVI during 2000-2022 is divided into five levels, the scale map is (b) and the spatial distribution map is (c).

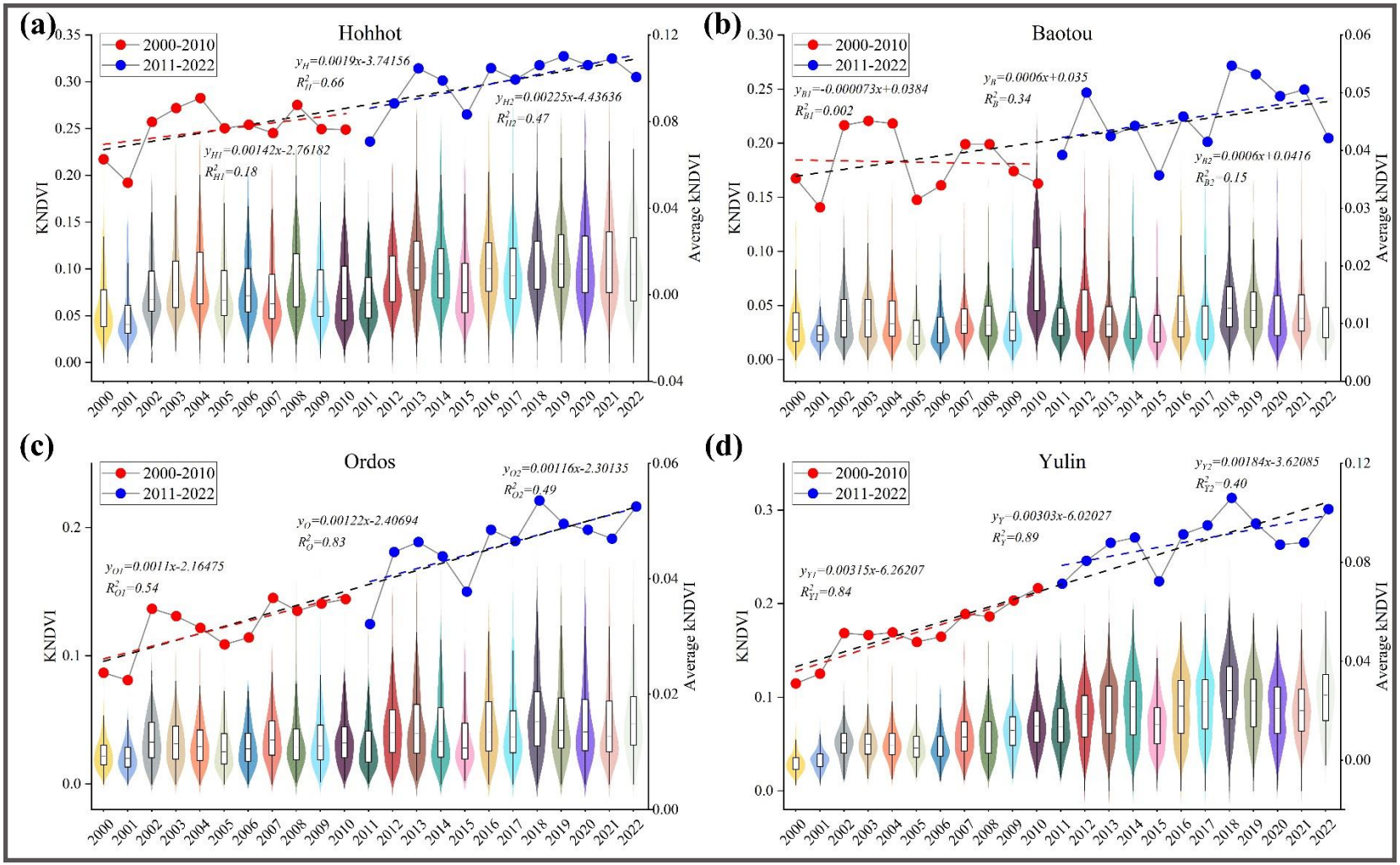

Figure S2. Temporal variation of kNDVI in Hohhot, Baotou, Ordos and Yulin.

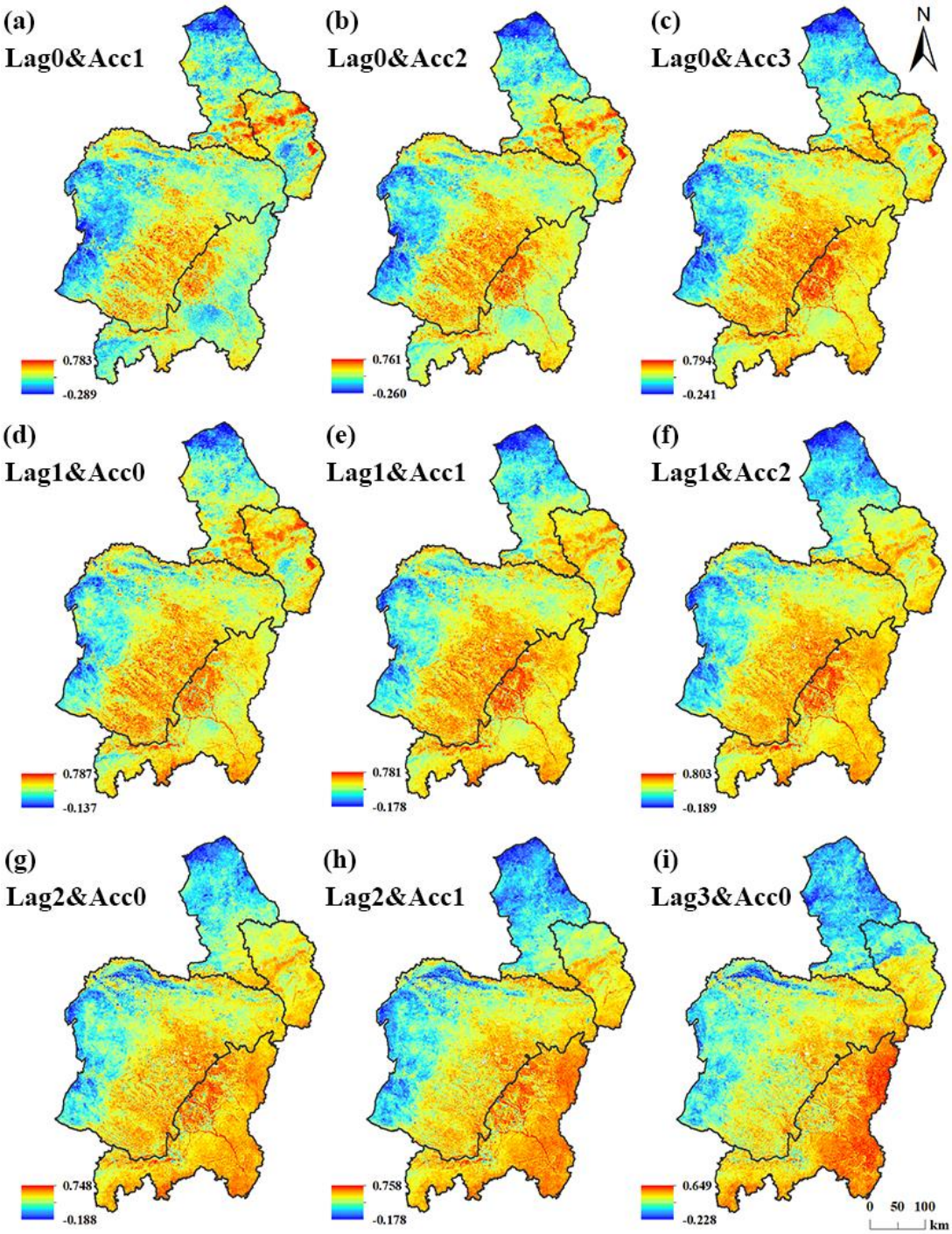

Figure S3. Second-order partial correlation coefficient between kNDVI and temperature under different combination of time-lag and accumulation effect.

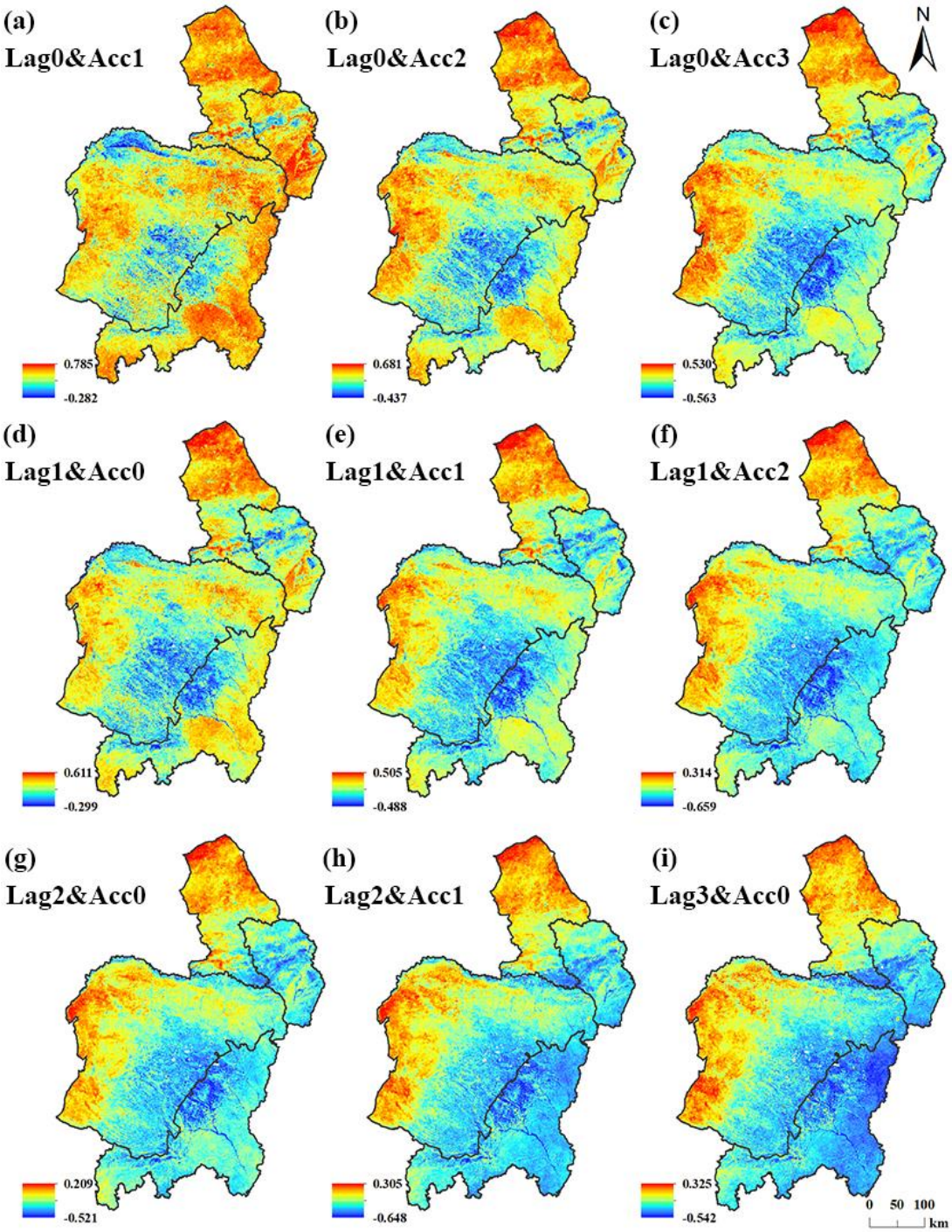

Figure S4. Second-order partial correlation coefficient between kNDVI and precipitation under different combination of time-lag and accumulation effect.

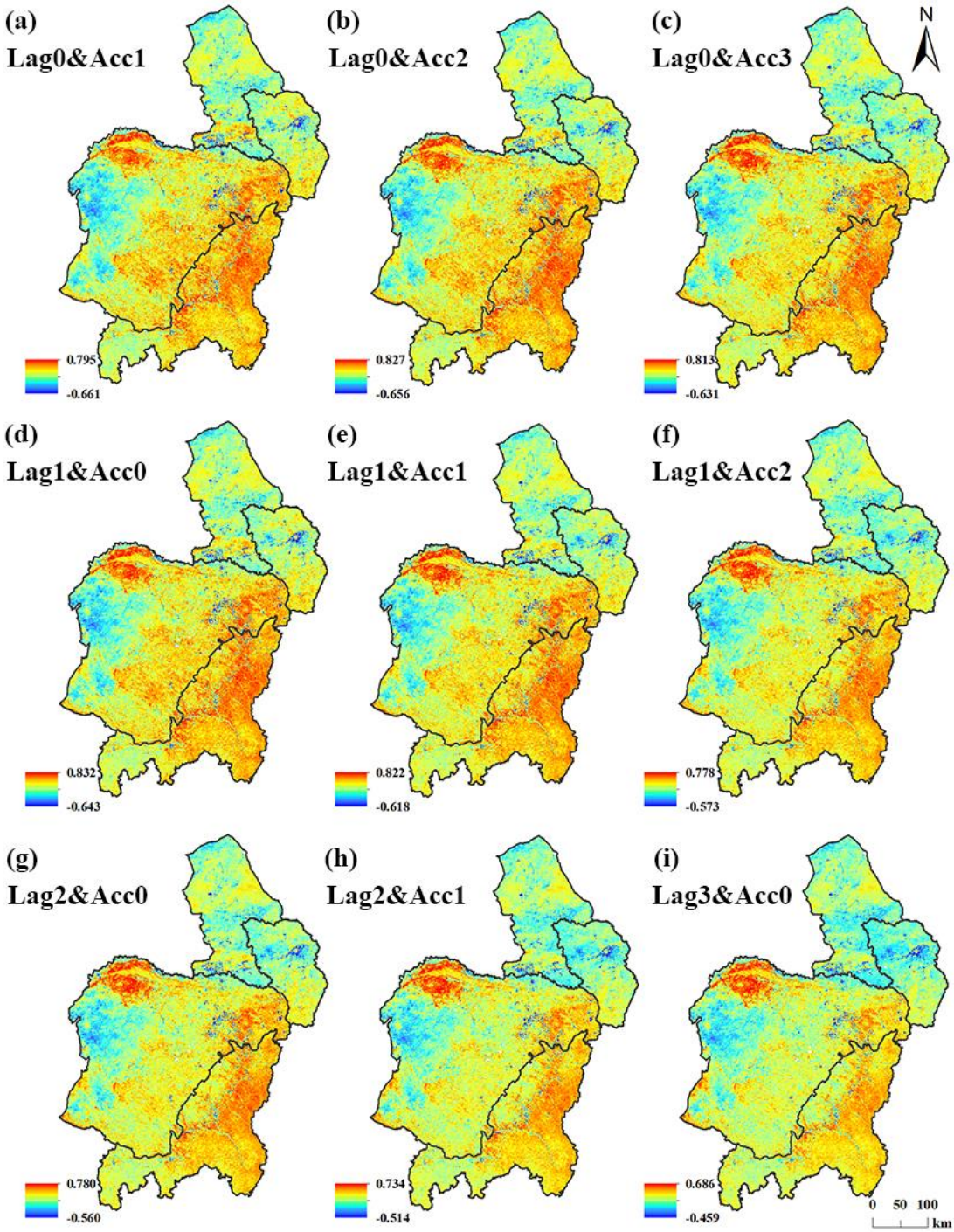

Figure S5. Second-order partial correlation coefficient between kNDVI and potential evapotranspiration under different combination of time-lag and accumulation effect.

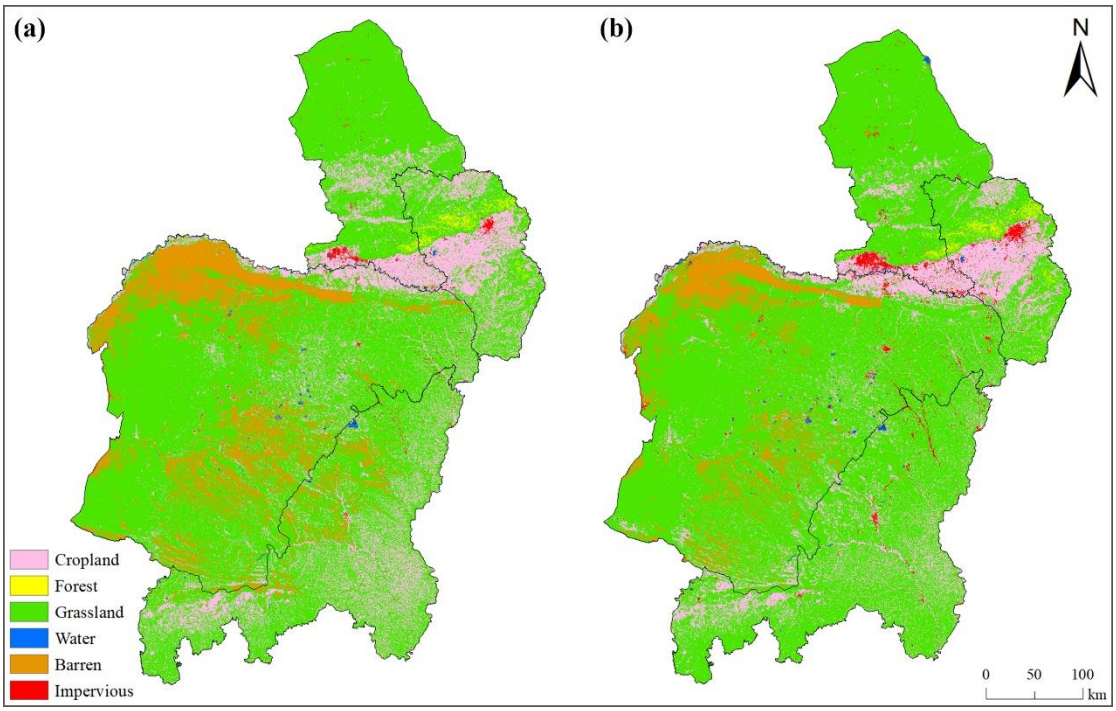

Figure S6. Land use of Hubao-Egyu urban agglomeration in 2000(a) and 2022(b).

Table S1. The lag and accumulation effects of vegetation on climate factors in different land use types, including the statistics of the proportion of four scenarios.

	P				T				PET			
Land use	No	Lag	Acc	LagAcc	No	Lag	Acc	LagAcc	No	Lag	Acc	LagAcc
Cropland	71.29	0.02	22.06	6.63	0.1	29.1	0.15	70.65	3.29	69.99	2.21	24.51
Forest	88.03	0	3.19	8.78	48.17	43.24	0	8.59	4.63	47.1	46.14	2.13
Grassland	51.24	0.08	42.89	5.79	1.29	58.49	0.16	40.06	2.25	70.53	3.14	24.08
Water	64.64	0.97	13.08	21.31	0.24	38.74	1.21	59.81	10.41	67.55	7.99	14.05
Barren	34.41	8.72	39.03	17.84	5.41	74.14	0.68	19.77	2.64	63.88	5.58	27.9
Impervious	68	0.47	20.8	10.73	0.43	42.58	0.28	56.71	16.69	59.59	7.54	16.18
Hubao-Egyu	53.55	0.69	38.87	6.89	1.68	54.79	0.2	43.33	2.68	69.65	3.52	24.15

Table S2. Contribution rate of CC (climate change) and HA (human activity) of vary land type under four temporal effects.

	CC				HA			
	No	Lag	Acc	LagAcc	No	Lag	Acc	LagAcc
Cropland	39.31	44.54	41.06	47.06	60.69	55.46	58.94	52.94
Forest	49.86	51.50	51.67	54.26	50.14	48.50	48.33	45.74
Grassland	42.59	48.38	44.71	49.12	57.41	51.62	55.29	50.88
Water	21.20	30.37	27.34	24.77	78.80	69.63	72.66	75.23
Barren	28.03	38.29	30.64	38.47	71.97	61.71	69.36	61.53
Impervious	36.48	40.11	38.12	42.71	63.52	59.89	61.88	57.29